Zeitschrift für Physikalische Chemie, **214**, 10, 1367−1381 (2000)

Ultrafast Proton-Transfer and Coherent Wavepacket Motion of Electronically Excited 1,8-Dihydroxyanthraquinone in Liquid Benzyl Alcohol Solution

By Jaydev Jethwa, Donald Ouw, Kathrin Winkler, Nicole Hartmann and Peter Vöhringer*

Max-Planck-Institute for Biophysical Chemistry, Biomolecular and Chemical Dynamics Group, Am Faßberg 11, D-37077 Göttingen, Germany

Dedicated to Prof. Dr. Dr. h. c. mult. Jürgen Troe on the occasion of his 60th birthday

(Received May 3, 2000; accepted June 5, 2000)

Femtochemistry / Wavepacket Dynamics / Proton Transfer

Ultrafast pump-probe experiments with a time-resolution of 30 fs have been carried out to explore the non-radiative relaxation dynamics of electronically excited 1,8-dihydroxyanthraquinone (DHAQ) in polar liquid solution. The results are discussed in terms of a Lippincott-Schroeder double-minimum potential along the proton-transfer reaction coordinate for the ground (S_0) and first excited singlet states (S_1) of DHAQ. The 400-nm pump-visible probe data reveal a strongly Stokes-shifted stimulated emission due to the proton-transferred 1,10-quinone configuration in the S_1-state. A dominant fraction of this stimulated emission appears instantaneously implying that cross-well excitation directly from the ground-state 9,10-quinone form into the excited-state 1,10-quinone configuration takes place. A smaller fraction of the stimulated emission appears delayed with a time constant of approximately 300 fs. This component may be due to proton-transfer in the S_1-state following optical excitation. Further, a transient absorption is observed on the red edge of the linear absorption spectrum of ground-state DHAQ due to higher-lying electronic states presumably from the 1,10-configuration. Periodic modulations of the transient absorption due to wavepacket motion in the 9,10-quinone form are partially consistent with previous fluorescence excitation spectra of the molecule taken under jet-cooled conditions.

1. Introduction

Proton-transfer processes are of considerable importance for research devoted to dynamics in disordered media with significant implications in

* Corresponding author. E-mail: pvoehri@gwdg.de

physics, chemistry, and biology [1−7]. As opposed to reactions involving large-amplitude motions such as dissociation [8−12] or isomerization reactions [13−16], proton-transfer dynamics involve the motion of one or more light hydrogen atoms. Thus, in addition to thermally activated barrier crossing, true quantum-effects such as tunneling may be involved in the reactive event [17−19]. As of today, the influence of a liquid environment on such kind of chemical processes is not fully understood [20−22]. Moreover, hydrogen-bonding is essential for the structure and the dynamics of a wide class of liquids whose static and dynamic properties profoundly affect the mechanisms, the time scales, and the outcome of chemical reactions [5, 23−27]. Finally, hydrogen-bond interactions play a fundamental role in determining the static structure of biological pigments as well as nucleic acids [28, 29]. Thus, elucidating the dynamics of proton motion may also improve our current understanding of the highly complex structure-dynamics-function relationships of these biological nano-machines.

Recently, ultrafast excited-state intramolecular proton-transfer (ESIPT) reactions in organic compounds have been studied quite extensively using time-resolved ultrafast spectroscopy [20, 30−36]. In general, ESIPT is initiated by optical excitation of the ‘keto’ (or ‘enol’) form which is the thermodynamically stable configuration in the electronic ground state. Optical excitation is followed by tautomerization into the ‘enol’ (or ‘keto’) form which is energetically favored in the electronically excited state and sometimes separated from the tautomer configuration by a potential barrier. The energetics in the ground and excited states result in a very pronounced Stokes shift of the spontaneous emission of the chromophore as described in the seminal work by Weller [37].

Gas phase studies or supersonic expansion experiments are capable of providing information with respect to the vibronic structure of both the electronic ground and excited states and the topology of the potential energy surfaces involved in the photo-induced ESIPT [38−40]. However, in condensed media, dynamic Stokes shift due to solvation and dynamic coupling of the solvent bath to the reaction coordinate may often obscure spectral signatures resulting from the reactive event [41]. These aspects are particularly crucial for ESIPT dynamics since reactant and product states are experimentally discernible through the spectral position of their emission [42].

In this paper, we present a time-resolved spectroscopic study of the nonradiative relaxation dynamics in the electronically excited state of 1,8-dihydroxyanthraquinone (DHAQ) in liquid solution following femtosecond optical excitation. DHAQ has been studied previously as a model system for ESIPT in supersonic jet expansions [40] as well as in Shpol’skii matrices at cryogenic temperatures [43−48]. From these efforts, a quantitative description of the potential energy surfaces relevant to ESIPT has emerged. In liquid solution, time-resolved fluorescence spectroscopy has been employed previously to elucidate the nonradiative relaxation dynamics of dihydoxy-

anthraquinones in polar and non-polar liquid solution [49]. However, the time resolution has been too poor to unambiguously resolve the primary step of ESIPT in this chromophore. Therefore, we felt that additional experiments with higher time-resolution were necessary to unambiguously identify the elementary proton-transfer step of DHAQ in liquid solution.

2. Experiment

Transient absorption measurements were carried out with a Ti : Sapphire laser/regenerative amplifier system capable of generating 800-nm, 30-fs optical pulses with energies as high as 4 μJ and repetition rates of 250 kHz. A portion (66%) of these amplified pulses were used to feed a collinearly pumped, white-light seeded optical parametric amplifier operating at a pump wavelength of 400 nm. Its output after compensation with a pair of $LAFN_{28}$ prisms consisted of a 250-kHz train of transform-limited 30-fs pulses centered at 610 nm with energies as high as 200 nJ. Approximately 20 nJ of these pulses served as probe pulses. Pump pulses were derived from the remaining 34% of the amplified 800-nm pulses by frequency doubling to 400 nm in a 0.5-mm thick type-I-BBO crystal. The 400-nm light was sent through a dispersive delay line consisting of two fused silica prisms to pre-compensate for any negative group velocity dispersion introduced by the pump-probe arrangement. The pulse duration of the pump pulses was also 30 fs as deduced from cross correlation measurements with the probe light.

The probe pulses were sent to a computer controlled delay line and were temporally and spatially overlapped in the sample with the pump pulses. The intensity of the probe light was measured with a photomultiplier whose output was directed to a digital lock-in amplifier (Stanford research, SR 830 DSP). The lock-in amplifier was referenced to a mechanical chopper modulating the pump beam at a frequency of 500 Hz.

The sample consisted of a free-flowing jet of DHAQ dissolved in benzyl alcohol with a thickness of 300 μm. DHAQ was received from Aldrich and further purified by silica gel column chromatography. The concentration was adjusted such that the sample had an optical density of 0.3 at 400 nm. Absorption spectra were recorded with a Shimadzu UV-160 UV/VIS spectrophotometer. Emission spectra were measured using a Fluorolog-3 Jobin-Yvon fluorescence spectrometer.

3. Results

The linear absorption and emission spectra of DHAQ dissolved in benzyl alcohol are displayed in Fig. 1. The absorption spectrum is rather structureless, however, weak shoulders on the high and low energy edges may indi-

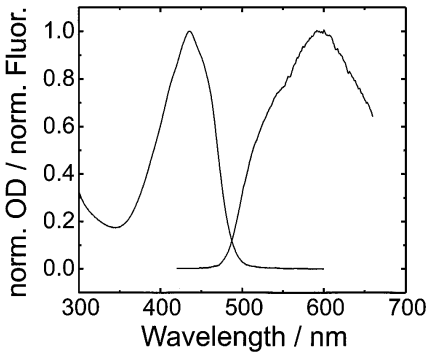

Fig. 1. Linear absorption and emission spectrum of DHAQ in benzyl alcohol.

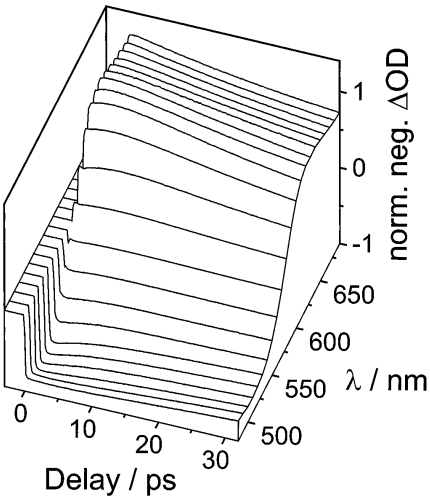

Fig. 2. Transient optical response of DHAQ in benzyl alcohol following 30-fs, 400-nm optical excitation.

cate some high-frequency vibronic sub-structure. It peaks around 435 nm and is very broad with a full width at half maximum of more than 4300 cm^{-1}. Similarly, the width of the emission spectrum is about 4800 cm^{-1}. The fluorescence is also rather structureless and the only feature that may be discernible corresponds to a high-energy shoulder around 520 nm. The emission peaks around 600 nm resulting in a total (peak-to-peak) Stokes shift of almost 8800 cm^{-1}.

Representative pump-probe transients following 400-nm, 30-fs excitation are displayed in Fig. 2 for delay times ranging from −5 ps to 32 ps

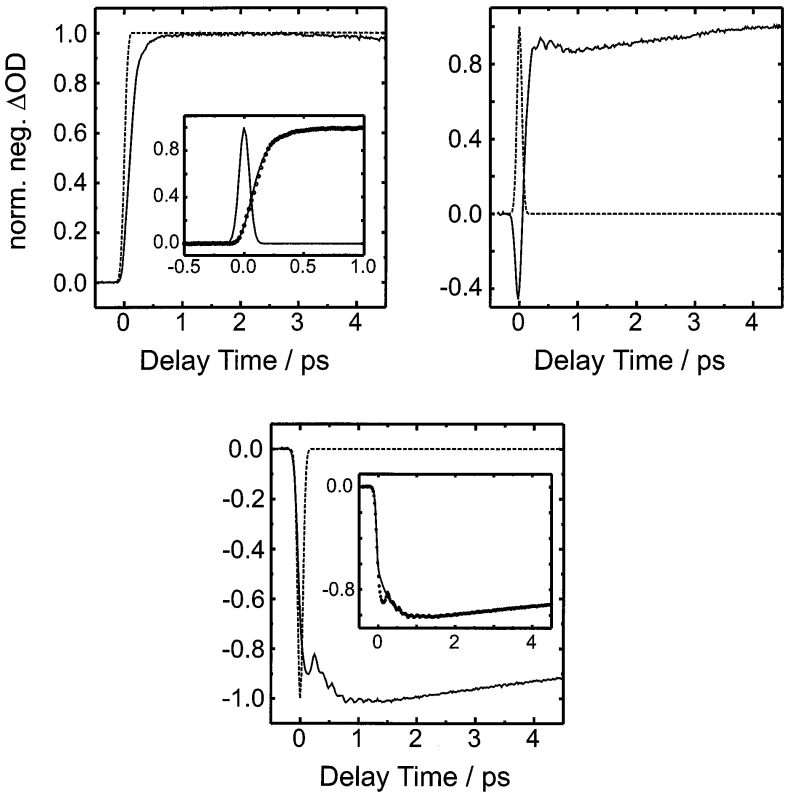

Fig. 3. Transient optical response of DHAQ in benzyl alcohol on short time scale following 30-fs, 400-nm optical excitation. Left panel: probe wavelength 640 nm. Right panel: probe wavelength 580 nm. Lower panel: probe wavelength 560 nm. The insets display the experimental data together with a fit to a double-exponential rise of the stimulated emission or transient absorption, respectively.

and for probe wavelengths between 490 nm and 690 nm. As expected, the dynamic spectra are dominated by stimulated fluorescence in the region of the low-energy tail of the spontaneous emission. Tuning the probe wavelength further into the blue results in a rapidly decreasing amplitude of the stimulated emission. Surprisingly, beyond 570 nm, the pump-probe transients are characterized by a very strong transient absorption. On longer delay times, both transient absorption and stimulated emission decay with the same time constant. This decay corresponds to the radiative lifetime, τ_{fl}, of the chromophore as reported previously by Barbara and coworkers [49]. Interestingly, a slower rise of the stimulated emission with small amplitude can be detected near the center of the spontaneous fluorescence spectrum

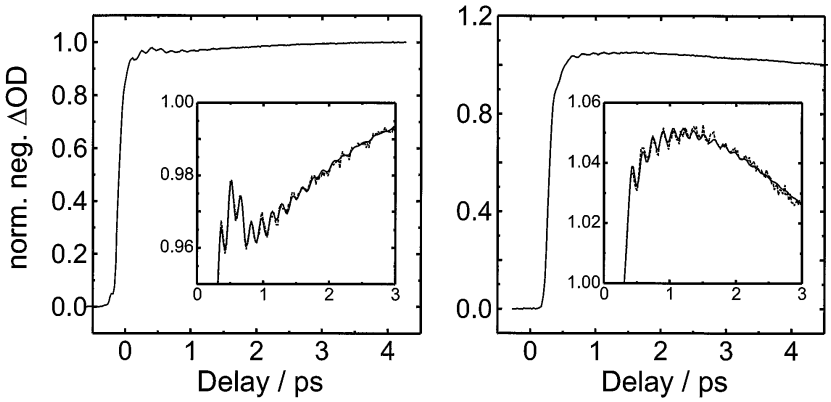

Fig. 4. Time-dependence of the stimulated emission recorded at the opposite edges of the stationary fluorescence spectrum of DHAQ in benzyl alcohol. Left panel: probe wavelength 590 nm. Right panel: probe wavelength 690 nm. The insets display the experimental data together with a fit to a double-exponential rise and a sum of exponentially damped cosinusoids according to the LPSVD analysis.

of DHAQ around 600 nm. Concurrently, a weak rise of the transient absorption is clearly observable at the bluest probe wavelength around 500 nm.

Inspection of the short-time dynamics of stimulated emission and transient absorption following 400-nm excitation of DHAQ is highly informative. Three normalized responses on a sub-5-ps time scale are displayed in Fig. 3. The transient recorded at 640 nm emphasizes the dynamic build-up of the stimulated emission. The probe wavelength is well located on the red edge of the linear emission spectrum and near the maximum of the stimulated emission. On the other hand, the 560 nm transient highlights the dynamic behavior of the stimulated absorption. In between, a probe wavelength of 580 nm was chosen which is located near the 'isobestic' point of the dynamic spectra where stimulated fluorescence and transient absorption are almost of equal amplitude.

The build-up of the stimulated emission can be fitted with a double exponential whose time constants are sub-100 fs and 300 fs (see inset). The faster component is not very well defined because its time constant comes close to our current time resolution. Simultaneously, the transient absorption displays an instantaneous rise as well as a slower component with a corresponding rise time of 330 fs. In addition, an exponentially decaying component with a time constant of 4 ps is necessary to reproduce the long-time tail of this transient for delays as large as 5 ps.

Finally, oscillatory modulations due to vibrational wavepacket dynamics are detected in both regions of stimulated emission and transient absorption, respectively. This behavior is emphasized in Fig. 4 for probe wavelengths

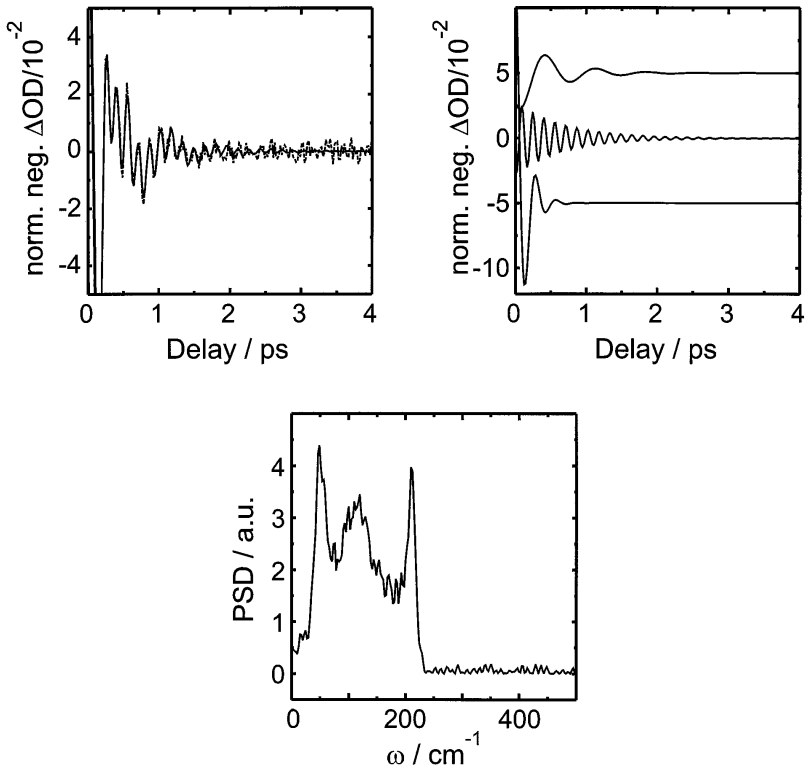

Fig. 5. Linear prediction singular value decomposition of an experimental pump-probe transient recorded at a probe wavelength of 590 nm. Left panel: experimental data after subtraction of all non-oscillatory components (dashed) and LPSVD-fit (solid). Right panel: individual frequency compoennts identified by the LPSVD-fit. Lower panel: Fourier spectrum of the experimental data after subtraction of all non-oscillatory components.

located at the opposite edges of the spontaneous fluorescence spectrum, i.e. for 590 nm and 690 nm. Information about the frequencies, ω, the amplitudes, A, the phase angles, ϕ, and the dephasing time constants, τ, can be obtained from linear prediction-singular value decomposition (LPSVD) of the pump-probe transients, S(t), after subtraction of the non-oscillatory (i.e. rising and decaying exponential) contributions [50−52]

$$S(t) = \sum_i A_i \cos\left[\omega_i t + \phi_i\right] \exp\left(-\frac{t}{\tau_i}\right). \quad (1)$$

Basically, such an LPSVD analysis reveals three frequency components oscillating with 47, 115, and 215 cm^{-1}. The low and high frequency contributions are only weakly damped with dephasing time constants of 520 fs

and 660 fs, respectively. In contrast, the intermediate frequency component is heavily damped and shows a time constant of 130 fs. The result of such an LPSVD analysis is exemplified in Fig. 5 for a probe wavelength of 590 nm.

To check for consistency, the pump-probe data can also be Fourier transformed, again after subtraction of all exponentials with zero frequency. The Fourier spectrum corresponding to the 590-nm data is displayed in Fig. 5. In accordance with the LPSVD analysis, three major components can be identified at frequencies of 50, 110, and 210 cm^{-1}. Again, low and high frequency contributions give rise to rather sharp features in the Fourier spectrum corresponding to weak damping with long dephasing times. In contrast, the contribution at intermediate frequency results in a broad feature analogous to very fast dephasing times and heavy damping. We note that these vibrational wavepackets are detected far away from the linear absorption spectrum of ground state DHAQ. Therefore, it is plausible to assign these features to coherent vibrational dynamics in the excited state induced by the ultrashort 400-nm excitation pulse.

4. Discussion

We begin this discussion by reviewing the spectroscopic properties of DHAQ as obtained from experiments performed under cryogenic temperatures and under isolated molecule conditions. Smulevich *et al.* reported fluorescence dispersion spectra of DHAQ in n-octane at 10 K which were used to reconstruct the vibrational structure of the chromophore in the electronic ground state [43−48]. Furthermore, they were able to measure the fluorescence excitation spectrum which gave insight as to the vibronic structure of the chromophore in the S_1 state. Interestingly, they detected a dual fluorescence originating from the proton transferred configuration of S_1 termed the 1,10-quinone configuration. A strongly red-shifted and a vibrationally unresolved emission was assigned to transitions leading back to the ground-state 1,10-quinone form. The ($S_0 \leftarrow S_1$) origin was detected at 21 112 cm^{-1} (i.e. 4052 cm^{-1} above the origin of the red-shifted emission). This origin together with well resolved vibrational progressions over more than 2000 cm^{-1} corresponds to cross-well emission from the 1,10-quinone form of S_1 to the 9,10-quinone configuration in the electronic ground state.

Smulevich *et al.* have also presented fluorescence excitation spectra of DHAQ dissolved in n-alkanes under cryogenic conditions [43−48]. In accordance with the dual emission described above, these authors found a dual excitation with two distinct origins. Most red-shifted, a sequence of sharp vibronic lines indicated the cross-well ($S_1 \leftarrow S_0$) transition whose origin coincides with the origin determined from their dispersed fluorescence data. A second origin could be located roughly 600 cm^{-1} above the

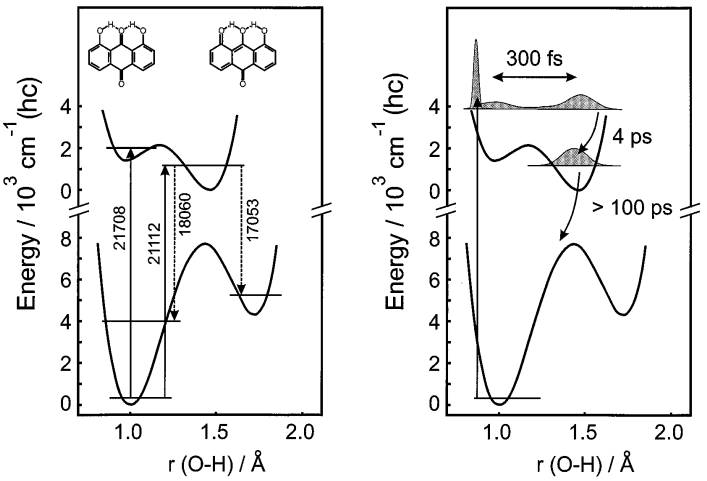

Fig. 6. Left panel: Lippincott-Schroeder potential for the ground and excited state of DHAQ following Smulevich and coworkers. Arrows with numbers indicate zero-zero transitions as observed in fluorescence dispersion and fluorescence excitation spectra under cryogenic temperatures. Right panel: Sketch of photoinduced dynamics and corresponding time scales following optical excitation at 400 nm.

origin of the cross-well ($S_1 \leftarrow S_0$) transition. For higher excitation energies, the spectrum became increasingly congested. Both, fluorescence dispersion and fluorescence excitation spectra were subsequenctly used to construct potential energy surfaces for the ground and excited state of DHAQ along the proton transfer coordinate. Using a Lippincott-Schroeder double-well model [53] for the potential energy functions of S_0 and S_1, it was possible to predict for a given O-O distance, the energy gaps and the intensity ratios between the two origins in both excitation and emission. In addition, the frequency shifts and the relative intensity changes of the origins upon deuteration was evaluated. It could be shown that the O-O distance of DHAQ is about 2.65 Å in the electronic ground state and by 0.15 Å slightly larger as compared to the excited state. This rather short O-O distance in the S_1-state implies that the equilibrium position of the 1,10-quinone form along the proton transfer coordinate (i.e. O-H distance) is shifted significantly towards the equilibrium position of the 9,10-quinone form of the ground state. The Lippincott-Schroeder potential energy curves for the ground and first excited singlet state of DHAQ according to Ref. [48] are reproduced in Fig. 6.

Gillispie *et al.* reported site-selected fluorescence dispersion and excitation spectra of DHAQ in n-octane Shpol'skii matrices as well as excitation spectra in an Argon free jet expansion [40]. A qualitative agreement of the excitation spectra under these rather different conditions was taken as evi-

dence for environment insensitive potential energy surfaces relevant to the photo-induced ESIPT dynamics of DHAQ. This aspect has tremendous impact for the time-resolved spectroscopic measurement reported here. It implies that a pronounced spectral evolution due to dynamic solvation following optical excitation of the chromophore cannot be expected. In fact, the long-time pump-probe transients displayed in Fig. 2 do not reveal any dramatic spectral shifts which may be connected to solvent reorganization.

In contrast to the Lippincott-Schroeder potential constructed in Ref. [48], Gillispie *et al.* concluded that the 9,10-quinone well in the S_1-state is too shallow to support a bound level in the OH-stretching vibration of the chromophore. They concluded that the potential energy surface of S_1 along the OH distance is effectively that of a distorted single minimum potential. However, by 600 cm^{-1} of excess vibrational energy above the global minimum of the S_1-state, the influence of the 9,10-quinone configuration is mainly a destruction of the harmonic nature of the reactive hypersurface.

Assuming that indeed the positions of the electronic origins remain unaffected in going from the gas phase to the liquid solution, an excitation wavelength of 400 nm as used in our pump-probe experiments will certainly lead to the excitation of both, the 1,10- and 9,10-quinone configurations of the electronically excited state. A 400-nm photon excites the chromophore to S_1 with roughly 3900 cm^{-1} of excess energy above the origin of the cross-well ($S_1 \leftarrow S_0$) transition and therefore, with roughly 3300 cm^{-1} of excess energy with respect to the Franck-Condon region in the 9,10-quinone well. Therefore, the instantaneously appearing portion of the strongly Stokes shifted stimulated emission is easily explained by direct cross-well excitations as discussed above. This interpretation also explains why previous time-resolved fluorescence experiments conducted by Barbara and coworkers with even higher excitation energies failed to observe the primary proton-transfer event [49].

However, our pump-probe data reveal a small fraction of stimulated emission which grows in with a time constant of 300 fs. It is tempting to assign this component to the primary proton-transfer process with motion of the hydrogen atom from the 9,10-quinone over to the 1,10-quinone form. Since it is not entirely clear whether or not there is a distinct barrier between the two excited-state tautomers, the detailed mechanism for proton transfer remains to be clarified. If indeed the potential well of the 9,10-quinone form is too flat to support a vibrational quantum in the OH-stretching vibration, it is more appropriate to associate the slow rise of the stimulated emission with a redistribution of amplitude along the hydrogen-transfer coordinate. An inspection of the Lippincott-Schroeder potentials in Fig. 6 suggests that a significant portion of the vibrationless ground-state wavefunction will be projected by a 400-nm pump pulse onto the excited state surface where the OH bond is even more compressed than in the energetically favored 1,10-quinone form of S_0. Subsequently, the wavepacket will spread according to

the local gradients of the S_1 leading to a rather broad equilibrium distribution of amplitude along R(OH). The proton transfer is then analogous to barrier-less relaxation dynamics with the final state being defined by the precise topology of the S_1 hypersurface. The stimulated emission is then a measure of those portions of the dynamically evolving wavepacket which can be projected by the probe pulse into the ground state 1,10-quinone well.

In the previous section, it was noticed that a 300-fs rising component can also be observed in transient absorption. Obviously, there are additional absorptive transitions to higher lying electronic states of DHAQ which are particularly sensitive to nuclear configurations of the chromophore resembling the 1,10-quinone form. Furthermore, an additional decay of the transient absorption with a time constant of roughly 4 ps was observed. The origin of these dynamics is somewhat unclear at the moment. However, it is possible that this decay is caused by vibrational energy relaxation into the surrounding solvent. It should be kept in mind that the excitation light provides the electronically excited chromophore with almost 4000 cm^{-1} of excess vibrational energy which will have to be released prior to radiative decay back to the ground state.

We now turn our attention to the coherent wavepacket dynamics seen in the pump-probe data on ultrafast time scales. Three major Fourier components below 250 cm^{-1} could be detected in both stimulated emission as well as transient absorption. It is interesting to compare their frequencies with high-resolution fluorescence excitation spectra observed at cryogenic temperatures. The most pronounced wavepacket was observed to oscillate with a frequency of about 215 cm^{-1}. Accidently, this frequency agrees rather well with the frequency of the CO bending vibration in the electronic ground state of DHAQ [46]. The oscillations observed in our pump-probe data, however, arise from the excited state since the ground state cannot contribute appreciably to the pump-induced optical density at such low probe energies. According to Smulevich *et al.* a vibrational band at 242 cm^{-1} can be seen above the second (i.e. high energy) origin of DHAQ. This feature was assigned to a skeletal in-plane deformation mode of the 9,10-quinone configuration of the electronically excited chromophore involving large amplitude motion of the two hydroxyl groups. Considering the large excess energy provided by the excitation pulse, the lower frequency observed in our pump-probe data may be rationalized by substantial anharmonic shifts. It has been speculated in the literature that such low-frequency vibrations play a key role in facilitating motion of the hydrogen atom during photoinduced ESIPT processes [30, 31, 35].

We do not wish to dwell on this issue in great detail since we believe that our pump-probe data are not conclusive enough to decide whether or not this particular large-amplitude motion of the OH-moieties represents a bottleneck for proton-transfer in the excited-state of DHAQ. However, we point out that the dephasing time constant for this particular mode is some-

what too large to be consistent with such a scenario. Interestingly, the dephasing time (600 fs) is roughly twice as large as the time constant (300 fs) for proton-transfer deduced from the delayed portion of the stimulated emission. If a barrier between the two excited state tautomers exists, then the 215-cm^{-1} wavepacket might indeed be assigned to optically induced coherent vibrational motion in an in-plane deformation mode of the 9,10-quinone configuration. Proton-transfer with motion towards the 1,10-quinone configuration on a time scale of roughly 300 fs should then contribute to vibrational dephasing of the reactant 9,10-quinone of S_1. Only if this low-frequency mode were purely harmonic, the coherent limit prevails and the apparent dephasing time should be twice the population relaxation time as observed. However, as discussed above, the wavepacket frequency indicates significant anharmonicities which should shorten the vibrational dephasing time substantially below 300 fs.

Surprisingly, the other two Fourier components with frequencies around 47 cm^{-1} and 115 cm^{-1} have been detected in the excitation spectra of DHAQ neither in Shpol'skii matrices nor in supersonic jet expansions. These excitation spectra have been recorded with a spectral resolution of about 1 cm^{-1}. Provided these modes carry sufficient oscillator strength, they should have been clearly visible if they were due to the bare chromophore. Consequently, we must conclude that these features are due to specific interactions with surrounding solvent molecules presumably through hydrogen bonding. Anharmonicities alone are not sufficient to explain wavepacket dynamics at such low frequencies since one would expect the dephasing time to increase dramatically with increasing vibrational excitation. Whereas this may still be the case for the 115 cm^{-1} feature, such an interpretation would certainly not hold anymore for the 47 cm^{-1} component.

Solvent modes which couple to the electronic transition dipole of the chromophore are usually overdamped [54]. Therefore, our finding of a rather weakly damped solvent or solute-solvent cluster mode is very surprising. Nevertheless, a coherent vibrational response of such solvent modes upon optical excitation of a chromophore has been observed before by Ernsting and coworkers in time-resolved Stokes shift data on the dynamic solvation of a fluorene dye dissolved in acetonitrile [55]. Further experiments using a number of different solvents are currently in progress to explore this intriguing aspect of solute-solvent interactions in more detail.

5. Conclusions

In conclusion, we have presented a time-resolved spectroscopic study of the non-radiative relaxation dynamics of 1,8-dihydroxyanthraquinone in benzyl alcohol solution. The data imply that proton transfer, or alternatively, redistribution of amplitude along the proton transfer coordinate following

400-nm optical excitation of DHAQ occur on a time scale of approximately 300 fs. At such high excitation energies, finer details regarding the dynamics of proton transfer are obscured due to a mixed preparation of both 1,10- and 9,10-quinone configurations of the electronically excited state of DHAQ. A more detailed study of the excitation energy dependence is currently in progress in our laboratory. Specifically, excitation at the red edge of the linear absorption spectrum of the chromophore near the ($S_1 \leftarrow S_0$) zero-zero transition will enable exclusive cross-well excitation of the 1,10-quinone form. It will then be possible to unambiguously monitor the backward proton-transfer to the 9,10-quinone configuration either through stimulated emission or through transient absorption provided the S_1 hypersurface allows for such dynamics.

Further, coherent vibrational wavepacket motion in the excited state of DHAQ was observed which is in agreement with low-frequency in-plane skeletal deformation modes involving large amplitude motion of the hydroxyl groups of the chromophore. These coherent vibrational dynamics are induced by the ultrashort excitation pulse presumably directly through excitation of the Franck-Condon region located in the vicinity of the 9,10-quinone configuration. We do not observe any evidence for coherent vibrational dynamics as a consequence of the reactive motion as concluded from similar studies on other intramolecular excited-state proton-transfer systems.

Acknowledgements

We thank Prof. Troe for his inspirational abilities as a mentor and teacher of physical chemistry. We consider ourselves fortunate to have enjoyed his fascination for science in the classroom and during our common research.

Financial support by the Deutsche Forschungsgemeinschaft through the Sonderforschungsbereich SFB 357 “Molekulare Mechanismen unimolekularer Reaktionen” is gratefully acknowledged.

References

1. D. Eisenberg and W. Kauzmann, *The structure and the properties of water*, Oxford University Press, Oxford (1969).
2. F. Franks, in F. Franks (Ed.), *Water. A comprehensive treatise*, Vol. 1, Plenum Press, New York (1972).
3. C. A. Angell, Ann. Rev. Phys. Chem. **34** (1983) 593.
4. E. W. Lang and H.-D. Lüdemann, Angew. Chem. Int. Eng. Ed. **21** (1982) 315.
5. I. Ohmine and S. Saito, Acc. Chem. Res. **32** (1999) 741.
6. D. Marx, M. E. Tuckerman, J. Hutter and M. Parrinello, Mol. Phys. **397** (1999) 601.
7. N. Agmon, Chem. Phys. Lett. **244** (1995) 456.
8. A. L. Harris, J. K. Brown and C. B. Harris, Ann. Rev. Phys. Chem. **39** (1988) 341.
9. U. Banin and S. Ruhman, J. Chem. Phys. **98** (1993) 4391.
10. T. Kühne and P. Vöhringer, J. Chem. Phys. **105** (1996) 10788.

11. P. K. Walhout, J. C. Alfano, K. A. M. Thakur and P. F. Barbara, J. Phys. Chem. **99** (1995) 7568.
12. H. Bürsing and P. Vöhringer, Phys. Chem. Chem. Phys. **2** (2000) 73.
13. J. Schroeder, J. Troe and P. Vöhringer, Z. Phys. Chem. **188** (1995) 287.
14. R. J. Sension, S. T. Repinec, A. Z. Szarka and R. M. Hochstrasser, J. Chem. Phys. **98** (1992) 6291.
15. J. Schroeder, J. Troe and P. Vöhringer, Chem. Phys. Lett. **203** (1993) 255.
16. J. Schroeder, D. Schwarzer, J. Troe and P. Vöhringer, Chem. Phys. Lett. **218** (1994) 43.
17. V. A. Benderskii, Russian Chemical Bulletin 48 **12** (1999) 2187.
18. J. L. Bjorkstam, Solid State Ionics **125** (1999) 13.
19. S. Lee and J. T. Hynes, Journal de Chimie Physique et de Physico-Chimie Biologique **93** (1996) 1783.
20. J. Dreyer and K. S. Peters, Ber. Bunsenges. Phys. Chem. **102** (1998) 493.
21. P. Purkayastha and N. Chattopadhyay, Phys. Chem. Chem. Phys. **2** (2000) 203.
22. S. Nagaoka and U. Nagashima, Chem. Phys. **206** (1996) 353.
23. S. Palese, L. Schilling, R. J. D. Miller, P. R. Staver and W. T. Lotshaw, J. Phys. Chem. **98** (1994) 6308.
24. S. Palese, J. T. Buontempo, L. Schilling, W. T. Lotshaw, Y. Tanimura, S. Mukamel and R. J. D. Miller, J. Phys. Chem. **98** (1994) 12466.
25. E. W. Castner, Y. J. Chang, Y. C. Chu and G. E. Walrafen, J. Chem. Phys. **102** (1995) 653.
26. M. Cho, G. R. Fleming, S. Saito, I. Ohmine and R. M. Stratt, J. Chem. Phys. **100** (1994) 6672.
27. S. Saito and I. Ohmine, J. Chem. Phys. **106** (1997) 4889.
28. G. A. Jeffrey and W. Saenger, *Hydrogen bonding in biological structures*, Springer-Verlag, Berlin (1991).
29. P. Schuster and P. Wolschann, Monatshefte Chem. **130** (1999) 947.
30. C. Chudoba, S. Lutgen, T. Jentzsch, E. Riedle, M. Woerner and T. Elsaesser, Chem. Phys. Lett. **240** (1995) 35.
31. C. Chudoba, E. Riedle, M. Pfeiffer and T. Elsaesser, Chem. Phys. Lett. **263** (1996) 622.
32. D. E. Folmer, L. Poth, E. S. Wisniewski and A. W. J. Castleman, Chem. Phys. Lett. **287** (1998) 1.
33. M. Glasbeek, D. Marks and H. Zhang, J. Lumin. **72** (1997) 832.
34. D. Marks, H. Zhang and M. Glasbeek, J. Lumin. **76-7** (1998) 52.
35. M. Pfeiffer, C. Chudoba, A. Lau, K. Lenz and T. Elsaesser, Laser Chem. **19** (1999) 101.
36. T. Sekikawa, T. Kobayashi and T. Inabe, J. Phys. Chem. **101** (1997) 644.
37. A. Weller, Naturwissenschaften **42** (1955) 175.
38. T. S. Zwier, Annual Review of Physical Chemistry **47** (1996) 205.
39. A. Muhlpfordt, U. Even and N. P. Ernsting, Chem. Phys. Lett. **263** (1996) 178.
40. G. D. Gillispie, N. Balakrishnan and M. Vangness, Chem. Phys. **136** (1989) 259.
41. A. B. Myers, Ann. Rev. Phys. Chem. **49** (1998) 267.
42. M. Novo, M. Mosquera and F. R. Prieto, J. Phys. Chem. **99** (1995) 14726.
43. G. Smulevich and M. P. Marzocchi, Chem. Phys. **94** (1985) 99.
44. M. P. Marzocchi, A. R. Mantini, M. Casu and G. Smulevich, J. Chem. Phys. **108** (1997) 534.
45. G. Smulevich, J. Chem. Phys. **82** (1985) 14.
46. G. Smulevich and M. P. Marzocchi, J. Chem. Phys. **108** (1998) 534.
47. G. Smulevich and M. P. Marzocchi, Chem. Phys. **105** (1986) 159.
48. G. Smulevich, P. Foggi, A. Feis and M. P. Marzocchi, J. Chem. Phys. **87** (1987) 5664.
49. S. R. Flom and P. F. Barbara, J. Phys. Chem. **89** (1985) 4489.

50. D. W. Tufts and R. Kumaresan, IEEE Trans. ASSP **30** (1982) 671.
51. R. Kumaresan and D. W. Tufts, IEEE Trans. ASSP **30** (1982) 833.
52. H. Barkhuijsen, R. De Beer, W. M. M. J. Bovee and D. van Ormondt, J. Magn. Res. **61** (1985) 465.
53. T. Saitoh, K. Mori and R. Itoh, Chem. Phys. **60** (1981) 161.
54. T. S. Yang, M. S. Chang, R. Chang, M. Hayashi, S. H. Lin, P. Vöhringer, W. Dietz and N. F. Scherer, J. Chem. Phys. **110** (1999) 12070.
55. J. Ruthmann, S. A. Kovalenko, N. P. Ernsting and D. Ouw, J. Chem. Phys. **109** (1998) 5466.